Appl. Phys. B 74 [Suppl.], S83–S88 (2002)
DOI: 10.1007/s00340-002-0906-8

Applied Physics B
Lasers and Optics

C. VARIN✉
M. PICHÉ

Acceleration of ultra-relativistic electrons using high-intensity TM_{01} laser beams

Centre d'Optique, Photonique et Laser, Université Laval, Québec, Canada

Received: 26 September 2001/
Revised version: 12 November 2001
Published online: 27 June 2002 • **© Springer-Verlag 2002**

ABSTRACT It is well known that very high axial – or longitudinal – electric fields can be obtained in vacuo using very intense focused laser beams. If these fields are in the transverse magnetic TM_{01} mode, very high gains in energy (exceeding 1 GeV) can be obtained if sufficiently energetic ultra-relativistic electrons (say 1 GeV) are injected on-axis and near the optimum phase. This energy gain is obtained even though the phase velocity of the axial component of the TM_{01} laser beam is greater than the vacuum velocity of light. The result is apparently related to the Gouy phase shift at focus.

PACS 41.75.Jv; 03.50.De; 41.20.Jb; 42.60.Jf

1 Introduction

From the very initial papers on laser-based acceleration schemes, it has been known that optical beams with a phase velocity less than the speed of light should be used in order to achieve velocity matching between the laser and particle beams (see [1]). According to Lawson [2], this is referred to as synchronous interaction. Since the use of extremely powerful laser beams inevitably implies serious material damage to any guiding or wave-slowing structure [3–6], an unbounded or free-space interaction is necessary. Known solutions of laser beams in free space, such as Bessel and Gaussian beams, have phase velocities higher than the speed of light. As a result, velocity matching cannot be obtained with these beams.

In many years of research on the subject of particle acceleration using high-intensity lasers, many acceleration schemes have been proposed: wave-slowing structures [3–6], wake fields in plasmas [7–9] and half-cycle or single-cycle pulses [10–12]. Simulations with laser beams in free space show that almost any laser beam of intensity smaller than 10^{16} W/cm^2 produces only a weak mean energy gain – a fraction of MeV – that is not even competitive with the standards of conventional accelerators (their typical energy gains per meter are about 50 MeV/m). On the other hand, we have found, through numerical simulations, that the theoretical energy gains obtained from very intense TM_{01} laser beams are promising, since they support the possibility of accelerating charged particles in free space, even though these beams have phase velocities exceeding the speed of light in vacuo. The objective of this paper is to describe this new approach to electron acceleration that takes advantage of the longitudinal field component of the laser beams under consideration.

Our paper is divided as follows. Section 2 deals with the field properties of the TM_{01} Laguerre–Gauss beam in free space. Section 3 examines the classical dynamics of a charged particle moving inside the electromagnetic field associated with a TM_{01} laser beam. Finally, Sect. 4 is a report of some of the numerical calculations we have performed, where cases of remarkable electron-energy gains stand out.

✉ Fax: +1-418/656-2623, E-mail: cvarin@phy.ulaval.ca

2 Field properties of the TM_{01} Laguerre–Gauss beam in free space

In this section, we proceed with a complete vectorial description of the electromagnetic field of the TM_{01} Laguerre–Gauss beam in free space. To characterize this particular beam, we will define its longitudinal electric field, its intensity profile and its phase velocity.

2.1 *Longitudinal electric field in free space*

The vectorial propagation of light in free space is governed by the four Maxwell equations. Assuming the wave propagation to be oriented along the z axis of a circular cylindrical coordinate system (r, ϕ, z), the electric field vector, $\boldsymbol{E}$, and the magnetic field vector, $\boldsymbol{H}$, can be expressed as follows:

$$\boldsymbol{H}(r,\phi,z,t)=\mathrm{Re}\left[\tilde{\boldsymbol{H}}(r,\phi,z,t)\,\mathrm{e}^{\mathrm{j}\omega t}\right], \quad (1)$$

$$\boldsymbol{E}(r,\phi,z,t)=\mathrm{Re}\left[\tilde{\boldsymbol{E}}(r,\phi,z,t)\,\mathrm{e}^{\mathrm{j}\omega t}\right]. \quad (2)$$

In this paper, we will make use of the well-known TM_{01} beam. We recall that this is the transverse magnetic mode ($H_z = 0$, $E_z \neq 0$), where '0' means that the components do not depend on the azimuthal angle ϕ and '1' that there is one zero for E_r (on the axis). The other field components are related to E_z by

the following equations [13]:

$$\tilde{H}_r = 0 \ , \tag{3}$$

$$\tilde{H}_\phi = -\frac{\mathrm{j}\omega\varepsilon_0}{\left(|\boldsymbol{k}|^2-\beta^2\right)}\frac{\partial\tilde{E}_z}{\partial r} \ , \tag{4}$$

$$\tilde{E}_r = -\frac{\mathrm{j}}{\left(|\boldsymbol{k}|^2-\beta^2\right)}\frac{\partial}{\partial z}\left[\, z\,\beta\,(z)\,\right]\frac{\partial\tilde{E}_z}{\partial r} \ , \tag{5}$$

$$\tilde{E}_\phi = 0 \ , \tag{6}$$

where ω is the angular frequency of the laser, $|\boldsymbol{k}| = 2\pi/\lambda$ is the magnitude of the wave vector expressed in terms of the wavelength λ, $\beta(z)$ is the projection of $\boldsymbol{k}$ on the z axis, ε_0 is the vacuum permittivity and $\mathrm{j} = \sqrt{-1}$. The complete mapping of the electromagnetic field profile of the TM_{01} beam is done by solving the source-free wave equation for the longitudinal field component $\tilde{E}_z$:

$$\nabla^2\tilde{E}_z + k^2\tilde{E}_z = 0 \ , \tag{7}$$

where k^2 stands for $|\boldsymbol{k}|^2$. Under the slowly varying envelope approximation, (7) can be modified in order to give the paraxial wave equation:

$$\nabla_T^2\tilde{E}_z - 2\mathrm{j}k\frac{\partial\tilde{E}_z}{\partial z} = 0 \ . \tag{8}$$

The lowest-order solution of (8) is expressed as a Gaussian longitudinal electric field that is a characteristic property of the TM_{01} Laguerre–Gauss beam [14, 15]:

$$\tilde{E}_z = E_0\frac{w_0}{w(z)}\,\exp\left(-\frac{r^2}{w^2(z)}\right)\mathrm{e}^{-\mathrm{j}(z-z_f)\beta(z)}\,\mathrm{e}^{-\mathrm{j}\phi_0'}, \tag{9}$$

$$\beta(z) = k\left[1+\frac{r^2}{2(z-z_f)R(z)}-\frac{\arctan\left(\frac{z-z_f}{z_0}\right)}{k(z-z_f)}\right], \tag{10}$$

$$w(z) = w_0\sqrt{1+\left(\frac{z-z_f}{z_0}\right)^2}, \tag{11}$$

$$R(z) = \left(z-z_f\right)+\frac{z_0^2}{\left(z-z_f\right)}, \tag{12}$$

$$z_0 = \frac{kw_0^2}{2}, \tag{13}$$

where E_0 is the longitudinal field amplitude, w_0 is the spot size at focus, $w(z)$ is the spot size at a given position along the z axis, ϕ_0' is the phase of the longitudinal electric field, z_f is the focus position, z_0 is the Rayleigh length and r is the transverse coordinate.

Using (4), (5), (9) and (10), the transverse electromagnetic field of the TM_{01} Laguerre–Gauss beam can be written, under the paraxial approximation, as

$$\tilde{H}_\phi \simeq \frac{2\mathrm{j}\omega\varepsilon_0}{\left(k^2-\beta^2\right)}\frac{r}{w^2(z)}\,\tilde{E}_z, \tag{14}$$

$$\tilde{E}_r \simeq \frac{2\mathrm{j}}{\left(k^2-\beta^2\right)}\frac{\partial}{\partial z}\left[\,\beta(z)\,(z-z_f)\,\right]\frac{r}{w^2(z)}\,\tilde{E}_z. \tag{15}$$

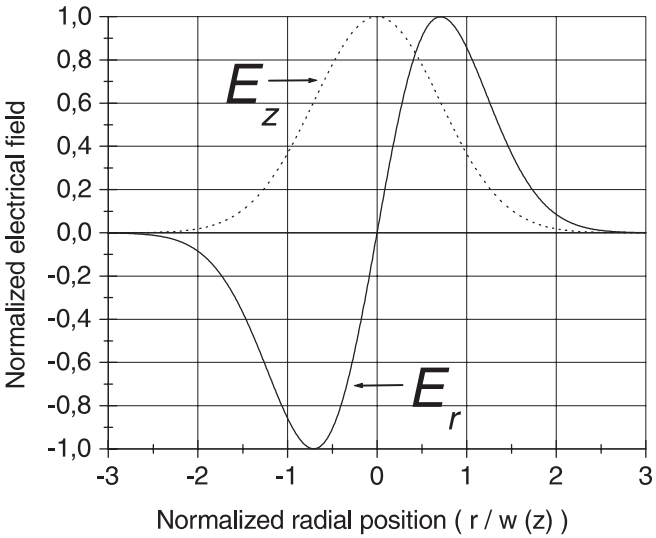

FIGURE 1 Transverse distribution (i.e. the r coordinate dependence of the field amplitude) of the transverse and longitudinal electrical fields (respectively E_r and E_z). Each field is self-normalized to give a maximum value of 1 and the radial position r has been normalized with respect to the beam spot size $w(z)$

At the center of the beam ($r = 0$), the transverse electric and magnetic fields are vanishing and the longitudinal electric field is at its maximum value. The transverse distributions of E_r and E_z are reproduced in Fig. 1.

2.2 *Poynting vector and intensity profile*

It is possible to find the intensity profile of the beam under consideration by taking the modulus of the average Poynting vector:

$$\begin{aligned} I(r,z) &= \frac{1}{2}\,\left|\mathrm{Re}\left[\boldsymbol{E}\times\boldsymbol{H}^*\right]\right| \\ &= \frac{1}{2}\,\left|\mathrm{Re}\left[-\tilde{E}_z\tilde{H}_\phi^*\,\hat{a}_r + \tilde{E}_r\tilde{H}_\phi^*\,\hat{a}_z\right]\right| \\ &= \frac{2\omega\varepsilon_0}{\left(k^2-\beta^2\right)}\frac{\partial}{\partial z}\left[\,\beta(z)\,(z-z_f)\,\right]\frac{r^2}{w^4(z)}\,\left|\tilde{E}_z\right|^2. \end{aligned} \tag{16}$$

If we perform $(\partial/\partial z)\left[\,\beta(z)\,(z-z_f)\,\right]$, (16) can be rewritten at focus (i.e. for $z = z_f$) as

$$I(r,z_f) = E_0^2\frac{k^2}{8\eta_0}\frac{\left[1-\frac{2}{k^2w_0^2}+\frac{2r^2}{k^2w_0^4}\right]}{\left[1-\frac{1}{k^2w_0^2}\right]^2}\,r^2\exp\left(-\frac{2r^2}{w_0^2}\right), \tag{17}$$

where η_0 is the intrinsic impedance of free space ($120\pi\ \Omega$). The intensity profile at focus $I(r, z_f)$ is shown in Fig. 2. It reaches its maximum value $I_{\max}$ at $r \simeq w_0/\sqrt{2}$, where $I_{\max}$ is given by

$$I_{\max} = E_0^2\frac{\mathrm{e}^{-1}}{16\eta_0}\frac{k^2w_0^2}{\left[1-\frac{1}{k^2w_0^2}\right]}. \tag{18}$$

The parameter $I_{\max}$ will be used later to 'calibrate' the value of the longitudinal field amplitude E_0.

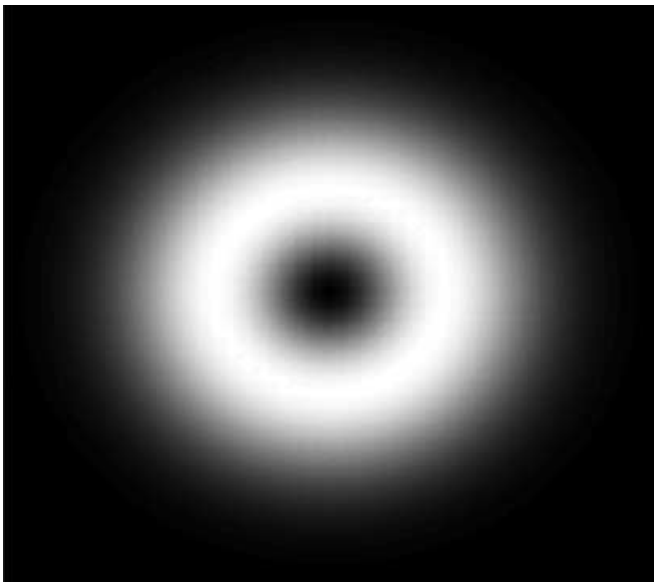

FIGURE 2 Intensity profile of the TM_{01} Laguerre–Gauss beam at focus. The center of the figure corresponds to $x = y = 0$

2.3 *Phase velocity in free space*

The phase velocity v_p can be easily derived from the previously defined $\beta(z)$ parameter (see (10)). For the problem under study, only the on-axis (i.e. $r = 0$) phase velocity is needed. If we take the phase to be stationary, we require that its differential be zero, i.e.

$$\mathrm{d}\phi(z) = \mathrm{d}\left[\omega t - kz + \arctan\left(\frac{z - z_f}{z_0}\right)\right] = 0 \ . \tag{19}$$

The phase velocity is then found to be given by

$$v_p = \frac{\mathrm{d}z}{\mathrm{d}t} = c\left[1 - \frac{1/kz_0}{1 + \left(\frac{z-z_f}{z_0}\right)^2}\right]^{-1} \ . \tag{20}$$

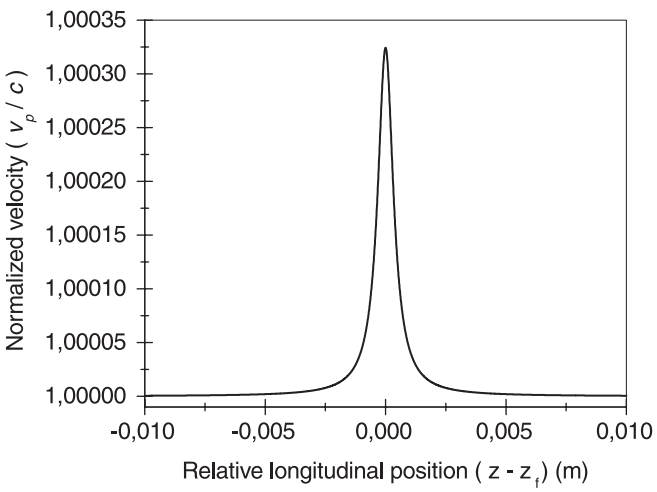

FIGURE 3 Normalized phase velocity of a TM_{01} Laguerre–Gauss beam near focus. The wavelength and the beam spot size have been set to $\lambda = 0.8\,\mu\mathrm{m}$ and $w_0 = 10\,\mu\mathrm{m}$

The parameter c is defined as the speed of light in vacuo. From (20), we can remark that $v_p > c$. The normalized phase velocity has been plotted in Fig. 3 for $\lambda = 0.8\,\mu\mathrm{m}$, $w_0 = 10\,\mu\mathrm{m}$ leading to $z_0 = 0.39\,\mathrm{mm}$. From that figure, it is possible to see that the phase velocity is very close to the speed of light except at focus. This behavior is due to the Gouy phase shift [16]. As we will see later, when a relativistic charged particle is injected at beam center ($r = 0$) with a trajectory parallel to the propagation axis of the laser beam ($v_z \simeq c$, $v_r = v_\phi = 0$), the phase shift of the TM_{01} Laguerre–Gauss beam gives rise to a peculiar on-axis dynamics.

3 Classical particle dynamics in a propagating electromagnetic field

This section examines the motion of a charged particle in an electromagnetic field. Our interest has been focused on the simplification of the four-dimensional equations of motion to a two-dimensional system and on the instantaneous radiation losses of an electron accelerated along a direction parallel to its initial velocity.

3.1 *Equations of motion*

The motion of a charged particle in an electromagnetic field is described by the Lorentz force equation:

$$\boldsymbol{F} = \frac{\mathrm{d}\boldsymbol{p}}{\mathrm{d}t} = q\left[\boldsymbol{E} + \boldsymbol{v} \times \boldsymbol{B}\right] \ . \tag{21}$$

The rate of the energy transfer from the field to the particle is given by

$$P = \frac{\mathrm{d}W}{\mathrm{d}t} = q\boldsymbol{E} \cdot \boldsymbol{v} \ . \tag{22}$$

One notes that $\boldsymbol{p}$ is the electron momentum, $\boldsymbol{E}$ is the electric field, $\boldsymbol{B}$ is the magnetic flux density, $\boldsymbol{v}$ is the particle velocity, q is the charge of the particle ($q = -e$ for the electron) and W is the particle total energy. From relativistic dynamics, we know that

$$\boldsymbol{p} = \gamma m \boldsymbol{v} = \frac{m\boldsymbol{v}}{\sqrt{1 - \frac{\boldsymbol{v}^2}{c^2}}}, \tag{23}$$

$$W = \gamma m c^2 = \frac{mc^2}{\sqrt{1 - \frac{\boldsymbol{v}^2}{c^2}}} \ , \tag{24}$$

where m is the particle rest mass.

The left-hand side of (21) can be expressed in term of $\boldsymbol{v}$ instead of $\boldsymbol{p}$. By doing this transformation, (21) and (22) can be written as

$$\frac{\mathrm{d}\boldsymbol{r}}{\mathrm{d}t} = \boldsymbol{v}, \tag{25}$$

$$\frac{\mathrm{d}\boldsymbol{v}}{\mathrm{d}t} = \frac{q}{\gamma m}\left[\boldsymbol{E} + \boldsymbol{v} \times \boldsymbol{B} - \frac{\boldsymbol{v}}{c^2}\left(\boldsymbol{E} \cdot \boldsymbol{v}\right)\right] \ . \tag{26}$$

In Sect. 1 we have described the properties of the TM_{01} Laguerre–Gauss beam; this type of beam has a dark spot at the center of its intensity profile. In this region, the amplitude of the transverse electric and magnetic fields is close to

zero as the longitudinal electric field reaches its maximum value. If a charged particle is injected at $r = 0$ with $v_r = v_\phi = 0$ and $v_z > 0$, the four-dimensional dynamics described by (25) and (26) can be simplified to a two-dimensional system expressed as follows:

$$\frac{\mathrm{d}z}{\mathrm{d}t} = v_z, \tag{27}$$

$$\frac{\mathrm{d}v_z}{\mathrm{d}t} = \frac{q}{m}\left[1 - \frac{v_z^2}{c^2}\right]^{\frac{3}{2}} E_z(r=0). \tag{28}$$

The on-axis real longitudinal electrical field E_z can be expressed from (9) as

$$E_z(r=0) = \mathrm{Re}\left[\tilde{E}_z(r=0)\,\mathrm{e}^{\,\mathrm{j}\omega t}\right] = \frac{E_0}{\sqrt{1+\left(\frac{z-z_f}{z_0}\right)^2}} \sin\left(\omega t - kz + \arctan\left(\frac{z-z_f}{z_0}\right) - \phi_0\right), \tag{29}$$

where ϕ_0 is the field initial phase.

3.2 *Radiation*

The instantaneous power radiated from an accelerated charge [17] is given by

$$P_{\mathrm{rad}} = \frac{2}{3}\,\frac{1}{4\pi\varepsilon_0}\,\frac{q^2}{m^2c^3}\,\gamma^2\left[\left(\frac{\mathrm{d}\boldsymbol{p}}{\mathrm{d}t}\right)^2 - \frac{1}{c^2}\left(\frac{\mathrm{d}W}{\mathrm{d}t}\right)^2\right] . \tag{30}$$

Following the procedure described in [17] for relativistic particles ($v_z \simeq c$), it is possible to obtain

$$\frac{P_{\mathrm{rad}}}{P} \simeq \frac{2}{3}\,\frac{1}{4\pi\varepsilon_0}\,\frac{q^2}{m^2c^4}\,\frac{\mathrm{d}W}{\mathrm{d}z} . \tag{31}$$

To achieve an efficient acceleration without excessive radiation losses, we must have

$$\frac{P_{\mathrm{rad}}}{P} \ll 1 \tag{32}$$

or

$$\frac{\mathrm{d}W}{\mathrm{d}z} \ll 4\pi\varepsilon_0\,\frac{3}{2}\,\frac{m^2c^4}{q^2} . \tag{33}$$

For an electron ($mc^2 = 0.511\,\mathrm{MeV}$ and $q = -1.602 \times 10^{-19}\,\mathrm{C}$), (33) can be evaluated to

$$\frac{\mathrm{d}W}{\mathrm{d}z} \ll 2.5 \times 10^{14}\,\mathrm{MeV/m} . \tag{34}$$

The acceleration gradient given by (34) would be produced by a longitudinal electric field of $2.5 \times 10^{20}\,\mathrm{V/m}$. Using (18) with $\lambda = 0.8\,\mu\mathrm{m}$ and $w_0 = 10\,\mu\mathrm{m}$, it is possible to show, for this proposed axial acceleration scheme, that radiation losses will not be significant as long as $I_{\max} \ll 10^{36}\,\mathrm{W/cm^2}$. We recall that such beam intensities are clearly out of reach for actual laser technology.

4 Acceleration by means of TM_{01} laser beam

The Gaussian beam, which possesses a finite energy, is of great physical interest. It has been used to describe numerous optical phenomena both in linear and nonlinear regimes. As a result of our recent calculations, we propose that TM_{01} Laguerre–Gauss beams, whose longitudinal component is Gaussian, have the properties required to obtain high energy gains for accelerated particles in vacuo: they can be focused far from any structure, they give the possibility to have a spatially limited longitudinal electric field in a transverse unbounded propagation and their Gouy phase shift of π at the focus can compensate for the electron slippage along their carrier wave. Since the focusing of a laser beam requires at least one lens (or any focusing element), the proposed acceleration scheme is not rigorously a free-space or an unbounded interaction. To the best of our knowledge, we think that an acceleration scheme using a TM_{01} Laguerre–Gauss beam could be realized with existing laser facilities.

Through numerical simulations, we have computed, for an electron, (27) and (28) where the longitudinal electric field is defined by (29). We have set z_f in the meter range (to avoid any material breakdown) and $w_0 \simeq 10\lambda$. We have studied the effect of the incident particle energy W_0, the peak intensity $I_{\max}$ and the phase of the accelerating field ϕ_0 on the energy gain $W - W_0$ for $\lambda_1 = 0.8\,\mu\mathrm{m}$ and $\lambda_2 = 10\,\mu\mathrm{m}$. One should not confuse z_0, the Rayleigh length (see (13)), with $z(t=0)$, the initial position of the particle. We have fixed the beginning of the interaction at $t = 0$ and $z = 0$. Following this definition, the effective field initial phase is $\phi_{\mathrm{eff}} = \phi_0 + \arctan(z_f/z_0)$.

Our numerical simulations have revealed that a number of different dynamical regimes are possible. Let us begin by considering the case of low-energy electrons ($W_0 \leq 10\,\mathrm{MeV}$) subject to the acceleration of TM_{01} laser beams of increasing intensity, as shown in Fig. 4. When the laser intensity is set at a value of $10^{18}\,\mathrm{W/cm^2}$ or lower, the electron energy is characterized by smooth periodic or quasi-periodic oscillations along the propagation axis. This behavior is due to the slippage of the electron inside the oscillating electric field; the initial speed of the electron being too small, it cannot experience a significant acceleration in the laser field. Under such circumstances, the electron sees a Doppler-shifted oscillating field whose amplitude is maximum at focus and vanishes far from it. As a result, the mean energy gain per cycle of acceleration is modest (from a fraction of MeV to $\approx 10\,\mathrm{MeV}$).

However, at extremely high values of laser intensity (top curve of Fig. 4), one sees that the electron energy no longer exhibits regular oscillations, as was the case for lower laser intensities. Due to the ultra-high longitudinal electric field, the electron energy can be pushed to large positive values over short distances. Still, the electron speed does not reach values sufficient to keep the electron in phase with the laser field. As a result, the electron slides in the optical cycle of the laser beam and loses the energy it had gained. Although the process repeats with an irregular period, one notes the nonsymmetrical character of the acceleration; oscillations of the electron energy take place about a mean value considerably different from the electron initial energy. This behavior can be interpreted as follows. When the electrons are accelerated, their energy allows them to stay in phase with the laser field for

a longer period than when they are decelerated. However, that effect is not sufficient to bring a significant net acceleration over the full interaction length with the laser beam.

When the electron initial energy W_0 is pushed to higher values, our computations predict that the electron dynamics undergoes radical changes, as shown in Fig. 5. To highlight the effect of W_0, we have kept the field intensity I_{max} to a fixed low value. As W_0 is increased from 10 MeV to 1 GeV, Fig. 5 reveals that the periodic oscillations of the electron energy evolve into a single-cycle feature. It means that ultra-relativistic electrons stay in phase with the laser field over one-half of the interaction length.

The strategy to obtain a net acceleration proceeds by combining a TM_{01} laser beam of extremely high intensity with ultra-relativistic electrons. Typical results are shown in Fig. 6, where the energy gain at the end of the interaction is plotted as a function of the phase of the field ϕ_0. Calculations were made over a long interaction length (10 m), given the extreme conditions that are used (one should bear in mind that such conditions are within the reach of experiments). Clearly, the top curve of Fig. 6 reveals that there are two values of the optical phase for which a clean acceleration is predicted for such values of the phase, the electron energy gain is enormous, exceeding the GeV range. At other values of the phase, the energy gain is vanishingly small. If the beam intensity is reduced, the energy gain decreases drastically (middle curve in Fig. 6) or virtually disappears (lower curve in Fig. 6).

To get some insight into the acceleration process, we have plotted the variation of the energy gain as a function of the propagation distance. Results are shown in Fig. 7 for two situations where a large energy gain is predicted; at $\lambda = 0.8\,\mu$m, the acceleration gradient is around 500 MeV/m, and for $\lambda = 10\,\mu$m it is as high as 4 GeV/m. Clearly, the curves shown in Fig. 7 indicate that most of the energy transfer from the laser beam to the electrons takes place around focus, as one would expect. Just before focus, electrons lose almost all their kinetic energy. From focus to the end of the interaction length, electrons stay in the same half-cycle of the laser field, experiencing a net acceleration. In other words, the electrons are slipping through the carrier of the field in such a way as to achieve velocity matching in the second half of the interaction length.

It should be noted that a modest acceleration can take place even beyond the focal zone. This feature is particularly striking in Fig. 7b. We attribute this behavior to the fact that the amplitude of the longitudinal field falls off as $(z - z_f)^{-1}$ away from focus, according to (9) and (11). When integrated over $(z - z_f)$ to compute the energy gain, one obtains a logarithmic divergence. Physically it means that the slow decrease of the longitudinal field amplitude over the propagation distance

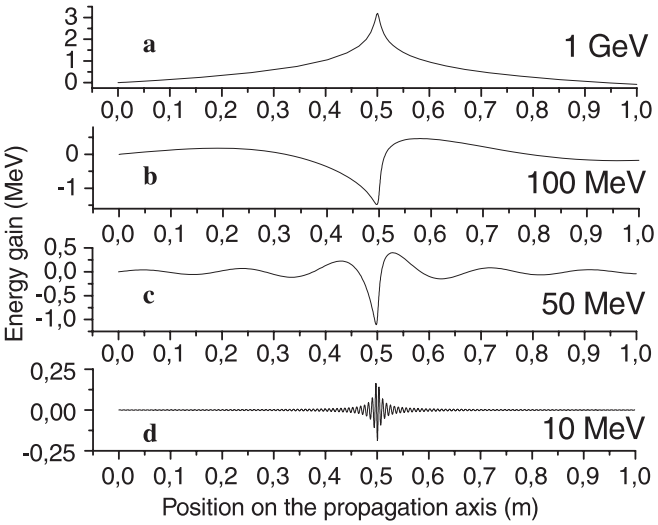

FIGURE 5 Energy gain $W - W_0$ along the propagation axis of a TM_{01} Laguerre–Gauss beam ($z_f = 50$ cm). The wavelength and the beam spot size have been set to $\lambda = 10\,\mu$m and $w_0 = 100\,\mu$m, the field initial phase ϕ_0 is zero and the intensity I_{max} has been set to 10^{12} W/cm^2. The electron initial energy W_0 is: **a** 1 GeV, **b** 100 MeV, **c** 50 MeV, and **d** 10 MeV

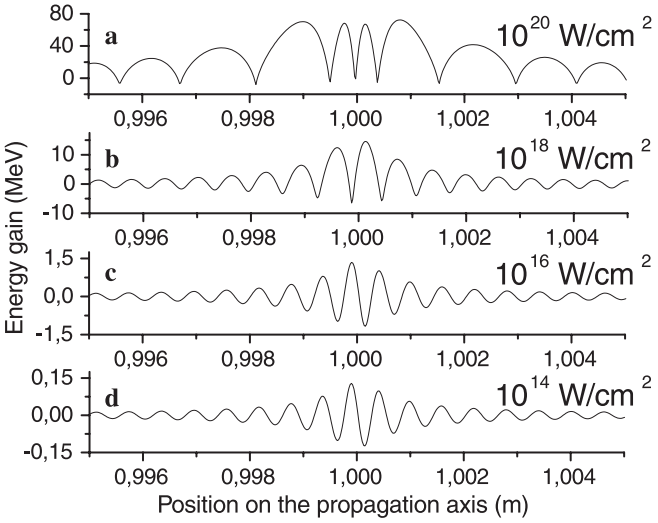

FIGURE 4 Energy gain $W - W_0$ along the propagation axis of a TM_{01} Laguerre–Gauss beam near the focus ($z_f = 1$ m). The wavelength and the beam spot size have been set to $\lambda = 0.8\,\mu$m and $w_0 = 10\,\mu$m, the field initial phase ϕ_0 is zero and the electron's initial energy W_0 is 10 MeV. The intensity I_{max} have been set to: **a** 10^{20} W/cm^2, **b** 10^{18} W/cm^2, **c** 10^{16} W/cm^2, and **d** 10^{14} W/cm^2

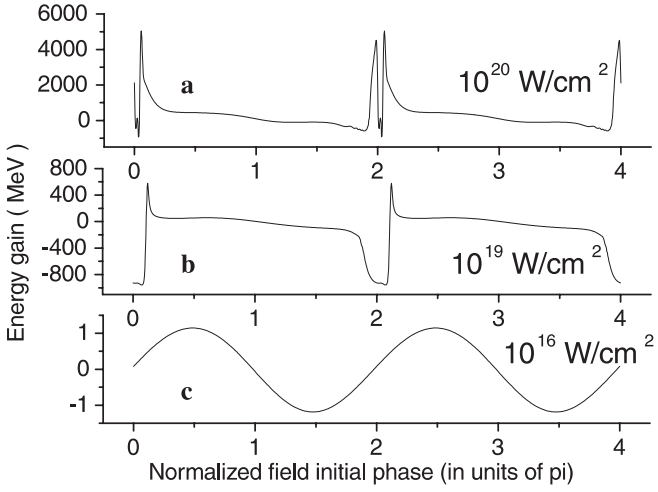

FIGURE 6 Energy gain $W - W_0$ along the propagation axis of a TM_{01} Laguerre–Gauss beam after a 10-meters interaction ($z_f = 3$ m). The wavelength and the beam spot size have been set to $\lambda = 0.8\,\mu$m and $w_0 = 10\,\mu$m. The electron initial energy W_0 is 1 GeV and the intensity I_{max} has been set to: **a** 10^{20} W/cm^2, **b** 10^{19} W/cm^2, and **c** 10^{16} W/cm^2

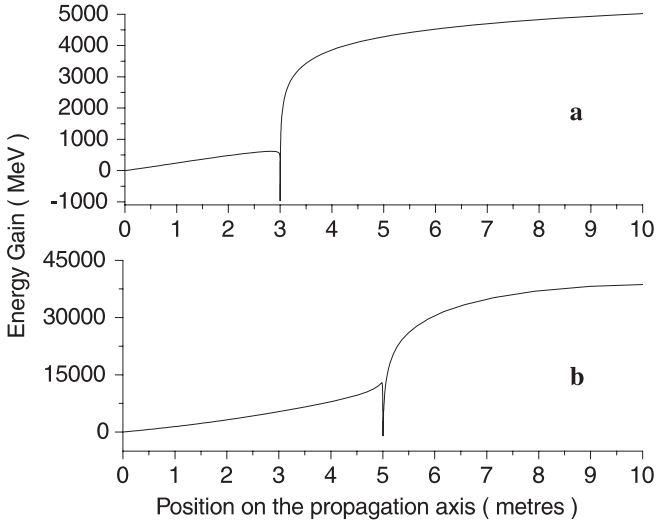

FIGURE 7 Energy gain $W - W_0$ along the propagation axis of a TM_{01} Laguerre–Gauss beam when the partial velocity matching conditions are satisfied. Parameters are $W_0 = 1$ GeV, $I_{max} = 10^{20}$ W/cm^2. For **a**: $\lambda = 0.8$ μm, $w_0 = 10$ μm, $z_f = 3$ m, and $\phi_0 = 0.054\,\pi$. For **b**: $\lambda = 10$ μm, $w_0 = 100$ μm, $z_f = 5$ m, and $\phi_0 = 0.095\,\pi$

makes this field component suitable for an efficient energy transfer from a TM_{01} laser beam to an electron beam.

5 Conclusion

In this paper we have proposed a new scheme for laser-based electron acceleration. We have shown that a TM_{01} laser beam possesses an axial longitudinal electrical field that, if sufficiently intense, can be used to transfer energies in the GeV range to correctly injected ultra-relativistic electrons, provided their injection energy is also in the range of a GeV and more. We have also demonstrated that radiation losses are not significant for the conditions under which experiments could be made.

We are presently extending our model to include the effects of the other field components of the laser beam and of noncollinear electron and beam trajectories. We are developing an understanding of the basic acceleration mechanism centered on the Gouy phase shift, which will be the object of future work. We are also investigating how the geometrical configuration of this scheme, which is linear, could be extended to a multistage operation leading to a high-performance (about 1 GeV/m) linear particle accelerator. This would imply a considerable reduction of the space requirements compared to existing linear accelerators.

ACKNOWLEDGEMENTS We wish to thank La Fondation J.-A. Vincent, the Natural Sciences and Engineering Research Council (Canada), Les Fonds pour la Formation de Chercheurs et l'aide à la Recherche (Québec) and the Canadian Institute for Photonic Innovations. We also thank the learned referee for numerous comments and suggestions.

REFERENCES

1 K. Shimoda: Appl. Opt. **1**, 33 (1962)
2 J.D. Lawson: IEEE Trans. Nucl. Sci. **26**, 4217 (1979)
3 J.R. Fontana, R.H. Pantell: J. Appl. Phys. **54**, 4285 (1983)
4 M.V. Federov, S.P. Goreslavsky, V.S. Letokhov: Phys. Rev. E **55**, 1015 (1997)
5 A. Tremaine, J. Rosenzweig, P. Schoessow: Phys. Rev. E **56**, 7204 (1997)
6 L.C. Steinhauer, R.D. Romea, D. Kimura: J. Appl. Phys. **83**, 5636 (1998)
7 P. Mora, T.M. Antonsen, Jr.: Phys. Rev. E **53**, R2068 (1996)
8 D. Gordon, K.C. Tzeng, C.E. Clayton, A.E. Dangor, V. Malka, K.A. Marsh, A. Modena, W.B. Mori, P. Muggli, Z. Najmudin, D. Neely, C. Danson, C. Joshi: Phys. Rev. Lett. **80**, 2133 (1998)
9 I.V. Pogorelsky: Nucl. Instrum. Methods Phys. Res. A **410**, 524 (1998)
10 R.W. Hellwarth, P. Nouchi: Phys. Rev. E **54**, 889 (1996)
11 B. Rau, T. Tajima, H. Hojo: Phys. Rev. Lett. **78**, 3310 (1997)
12 K.-J. Kim, K.T. MacDonald, G.V. Stupakov, M.S. Zolotorev: Phys. Rev. Lett. **84**, 3210 (2000)
13 D.K. Cheng: *Field and Wave Electromagnetics* (Addison Wesley, New-York 1992) p. 523
14 A.E. Siegman: *Lasers* (University Science Books, Sausalito, California 1986) p. 689
15 P.-A. Bélanger, P. Mathieu: Opt. Commun. **67**, 396 (1988)
16 S. Feng, H.G. Winful: Opt. Lett. **26**, 485 (2001)
17 D.J. Jackson: *Classical Electrodynamics* (Wiley, New York 1999 p. 666